Journal of Applied Polymer Science

Synthesis of biodegradable polyurethanes chain-extended with (2*S*)-bis(2-hydroxypropyl) 2-aminopentane dioate

Eda Ayse Aksoy,[1,2] Gulce Taskor,[1,3] Merve Gultekinoglu,[1,4] Filiz Kara,[1] Kezban Ulubayram [1,2,3,4]

[1]Department of Basic Pharmaceutical Sciences, Faculty of Pharmacy, Hacettepe University, Ankara 06100, Turkey

[2]Polymer Science and Technology Division, Institute for Graduate Studies in Science and Engineering, Hacettepe University, Ankara 06640, Turkey

[3]Nanotechnology and Nanomedicine Division, Institute for Graduate Studies in Science and Engineering, Hacettepe University, Ankara 06640, Turkey

[4]Bioengineering Division, Institute for Graduate Studies in Science and Engineering, Hacettepe University, Ankara 06640, Turkey

Correspondence to: K. Ulubayram (E-mail: ukezban@hacettepe.edu.tr)

ABSTRACT: Polyurethanes (PUs) are the most widely used polymers because of their biocompatibility, tunable mechanical properties, and chemical versatility. In this study, a two-step condensation polymerization of polycaprolactone diol and hexamethylene diisocyanate was carried out, and a glutamic acid ester derivative, (2*S*)-bis(2-hydroxypropyl) 2-aminopentane dioate (HPAP), was used as a new chain extender to accelerate the biodegradation properties of PU. HPAP was synthesized by the Fischer esterification of L-glutamic acid. The chemical structure of HPAP was confirmed by high-resolution mass spectroscopy and *m/z* (EI) was found to be 264.1447 [calculated value = 264.1443 for $C_{11}H_{21}NO_6$ (M^+)]. The Berry plot of static light-scattering measurements showed that PU–HPAP had a weight-average molecular weight and radius of gyration of 33,100 g/mol and 1420 nm, respectively. The presence of HPAP in the PU structure facilitated hydrogen bonding between the polymer chains and increased the glass-transition temperature from −56 °C (PU) to −50 °C (PU–HPAP). PU–HPAP showed the highest hydrophilicity and surface free energy among all of samples, and this accelerated the *in vitro* biodegradation period via surface erosion. In addition, PU–HPAP did not show any cytotoxic effects on the L929 cells. A new biodegradable and biocompatible PU–HPAP was obtained as candidate for tissue engineering applications. © 2017 Wiley Periodicals, Inc. J. Appl. Polym. Sci. **2018**, *135*, 45764.

KEYWORDS: biocompatibility; degradation; polyurethanes

Received 28 March 2017; accepted 7 September 2017

DOI: 10.1002/app.45764

INTRODUCTION

Since the 1990s, continuous efforts have been made to develop novel biodegradable polymers as supporting materials for tissue engineering and regenerative medicine applications. Researchers have used wide diversity of polysaccharide- and protein-based biopolymers, including alginate, chitosan, starch, cellulose, collagen, and silk fibroin, for their bioresorbability[1–3] and synthetic biodegradable polymers;, including polyesters,[4] polyanhydrates, polyurethanes (PUs)[5,6] and their blends[7] and copolymers, as biodegradable matrices.[8] Among all of these biodegradable polymers, PUs possess the advantages of condensation polymerization; they offer a wide diversity of chemical and mechanical properties and adequate biocompatibility via the selection of monomers, chain extenders, and polymerization parameters. The PU chemical structure is composed of not only urethane groups but also many other groups, including ether, ester, urea, allophanate, and biuret groups.[9] The chemical structure of the monomers and chain extenders provide thermodynamically immiscible soft and hard segments in PU at a macromolecular level. This phase separation consequently governs the final properties of the PU products.[10] PUs can be processed in film, sponge, and fiber forms according to the requirements in biomedical areas.[11,12] Also, PU linkages offer surface functionality, which provides critical binding sides for further surface-modification applications.[12–14]

For new-generation biomaterials, tissue supports, and tissue engineering scaffolds, the biodegradation of the polymer matrix is crucial. In biological environment, the bulk and surface chemistry of the polymer determine whether it is biodegradable, bioerodable, bioabsorbable, or bioresorbable.[15] The biodegradation process depends on the molecular weight, polydispersity, crystallinity, tacticity, hydrophilic and hydrophobic functional groups, and susceptibility under *in vivo* conditions.[16] For PUs, the biodegradation period and degradation products can be

© 2017 Wiley Periodicals, Inc.

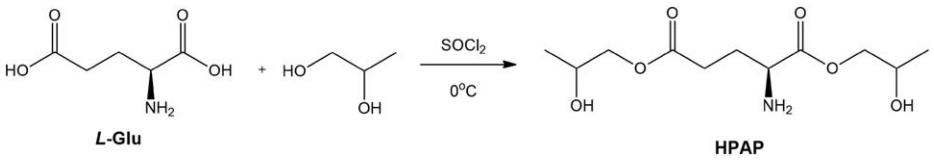


Figure 1. Synthesis reaction for HPAP.

tailored by monomer selection and polymerization parameters. The soft segments or the hard segments can both mediate the biodegradation of PUs. Soft-segment degradation occurs through ester-bond hydrolysis, and the degradation period can be tailored from weeks to years through the choice of polyester polyols, such as poly(glycolic acid) (PGA), poly(lactic acid), and poly(ε-caprolactone) diol or triols.[1,17] Generally, the hard segment degrades much more slowly than the soft segment because of the urethane linkages, which are much less susceptible to hydrolytic degradation.[17] In these cases, diisocyanate- and hydrocarbon-based diols or diamines as chain extenders (OH—R—OH, NH_2—R—NH_2 where R is a hydrocarbon, e.g., 1,4-butanediol) form the hard segment of PU and provide extra strength because of the hydrogen bonding between urethane linkages; this results in the retardation of hydrolytic degradation.

In this study, we aimed to use a novel chain extender, (2*S*)-bis(2-hydroxypropyl) 2-aminopentane dioate (HPAP), which is a glutamic acid ester derivative, to accelerate the biodegradation period of PU. Glutamic acid was used as the starting compound of HPAP. Its asymmetric chiral carbon has levorotatory (L) and dextrorotatory (D) forms, where the L isomer [L-glutamic acid (L-Glu)] occurs mostly in nature. L-Glu is one of the most important amino acids, with a wide range of applications, including in biodegradable polymers,[18] therapeutics,[19] and neurotransmitter substances.[20] This feature makes the derivatives of L-Glu a motif for generating glutamic acid ester based chain extenders, which may be an important building block for the design of biodegradable PUs.

In the literature, chain extenders, which are susceptible to hydrolytic degradation, have been reported to trigger the biodegradation of PUs. Skarja and Woodhouse[21,22] reported that amino acid based chain extenders, which were synthesized by a diesterification reaction between L-phenylalanine and 1,4-cyclohexane dimethanol, affected the physicochemical and degradation characteristics of PU. Chan-Chan *et al.*[23] synthesized a family of degradable segmented poly(urea)urethanes with amino acids (L-arginine, glycine and L-aspartic acid) as chain extenders and studied degradation in phosphate-buffered saline (PBS) and acidic, alkaline, and oxidative media. In the literature, DL-lactic acid–ethylene glycol based hydrolysable ester,[5] the amino acid antioxidant glutathione,[24] water,[25] aminated phosphorycholine,[5] aniline pentamer,[26] 2,2-(methylimino)diethanol,[27] 2,6-pyridinedimethanol,[28] dithioerythritol,[29] L-tyrosine-based diphenolic dipeptides,[30] and desaminotyrosyl tyrosine hexyl ester[30] have been reported as chain extenders that accelerate the biodegradation period of PUs. In recent years, isosorbide[31] was used as a chain extender in biodegradable PUs, and it decreased the cross-linking density of the polymer; this is an important parameter for biodegradation. On the other side, a fluoro chain extender, 2,2,3,3,4,4,5,5,-octafluoro-1,6-hexanediol, was incorporated into a biodegradable PU matrix, and polymers that were less degradable than pristine PU were obtained.[32]

In this study, first, PU prepolymers were synthesized by the condensation polymerization of polycaprolactone (PCL) diol and hexamethylene diisocyanate (HDI), and in the second step, a PU prepolymer was chain-extended with a glutamic acid ester derivative, HPAP. HPAP, a new glutamic acid derivative chain extender, was synthesized and introduced into PU to increase the biodegradation rate and also provide biocompatible degradation products. For this purpose, L-Glu was chosen for the starting compound, and HPAP was synthesized by the Fischer esterification method from L-Glu. Detailed characterizations were performed with high-resolution mass spectroscopy (HRMS) and NMR spectrometry to correlate the chemical structure of HPAP. Additionally, both non-chain-extended PUs and L-Glu containing PUs were also synthesized as pristine samples. The chemical characterizations of the PU–HPAP and pristine samples were performed with NMR and attenuated total reflectance (ATR)–Fourier transform infrared (FTIR) spectrometers. Molecular weight determinations were done by static light scattering (SLS); the thermal transitions and thermal degradation properties of the polymers were examined with differential scanning calorimetry (DSC) and thermogravimetric analysis (TGA), respectively. Also, *in vitro* degradation and *in vitro* cytotoxicity test studies were performed for the newly synthesized polymers.

EXPERIMENTAL

Materials

L-Glu (99%), 1,2-propane diol (99%), and thionyl chloride ($SOCl_2$; 99%) were obtained from Sigma-Aldrich Co. The purity of the chain extender was assessed by thin-layer chromatography (Merck silica gel plates, type 60 F254). Ninhydrin was purchased from Sigma-Aldrich Co. PCL diol was purchased from Sigma-Aldrich Co., and it had a quoted number-average molecular weight of 2000. HDI (99%) and tin(II) 2-ethyl hexanoate (92.5–100%) were supplied from Sigma-Aldrich Co. The solvents, including *N*,*N*-dimethylformamide (DMF) (99%), methanol (99.9%), and $CHCl_3$ ($CHCl_3$; 99%), were CP grade and were obtained from Sigma-Aldrich Co. Before use, DMF was stored in the presence of a 4 Å molecular sieve. PBS, Dulbecco's modified Eagle's medium), fetal bovine serum, (4,5-dimethyl thiazol-2-yl)-2,5-diphenyl tetrazolium bromide (MTT), L-glutamine, and penicillin/streptomycin was obtained from Biochrom (Germany). EtOH (99.5%), propan-2-ol (99.5%), and hydrochloric acid (HCl; 37%) were purchased from Merck (Germany). Lipase from porcine pancreas type II was purchased from Sigma-Aldrich (Germany).

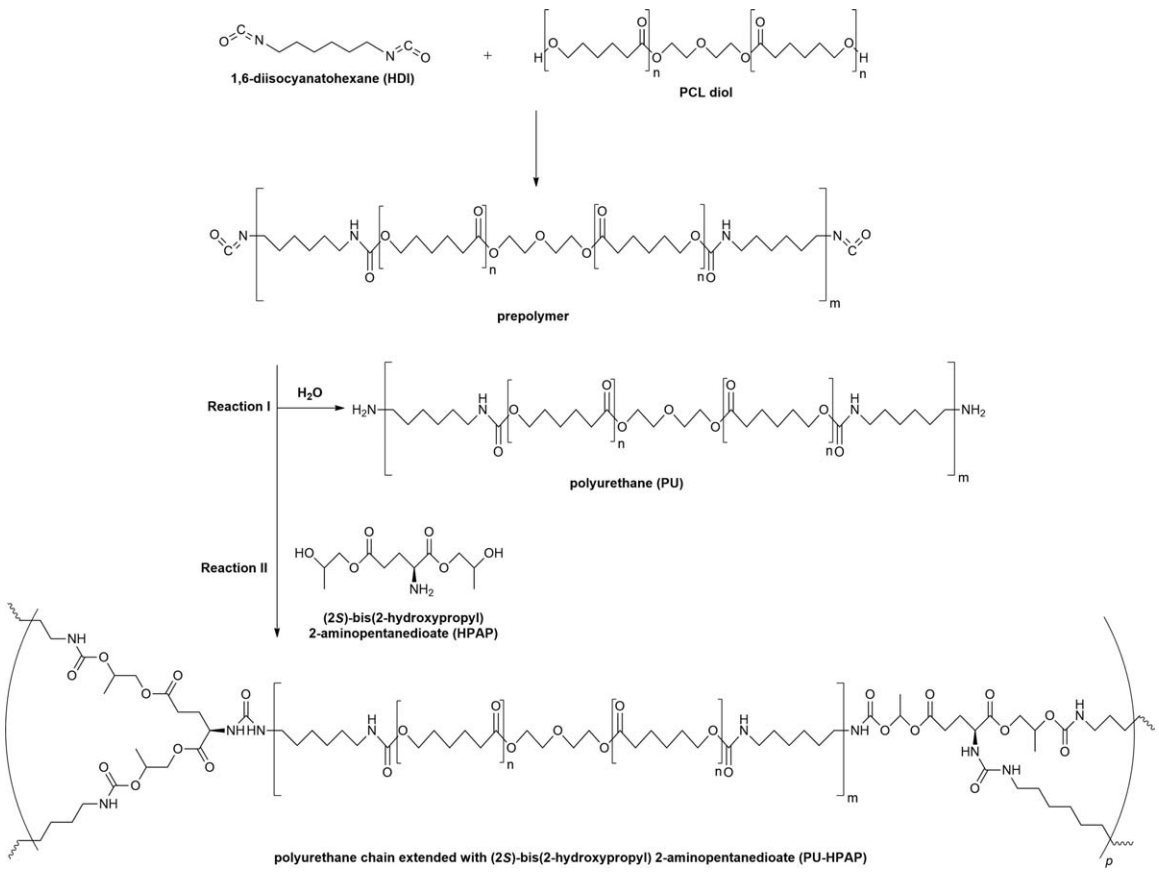


Figure 2. Schematic representation of the biodegradable PU and PU–HPAP chain-extender synthesis reaction steps.

Synthesis of HPAP

HPAP was synthesized by the Fischer esterification method (Figure 1). Briefly, $SOCl_2$ (2.74 mL, 37.5 mmol, 5 equiv) was added dropwise to 1,2-propane diol (40 mL) at 0 °C for 15 min. After that, 15 mmol of L-Glu was introduced into this mixture, which was stirred at room temperature for 168 h. Thin-layer chromatography with 5:1 v/v methanol–$CHCl_3$ indicated the complete disappearance of amino acid. The product was purified by distillation at a reduced pressure (162 °C) to obtain the novel chain-extender compound (HPAP) as a yellow liquid at 85% yield.

Synthesis of PU with HPAP

In a round-bottom flask equipped with a magnetic stirrer, PCL diol (10.00 g, 5.0 mmol, 1.0 equiv) dissolved in anhydrous DMF (50 mL) was reacted with HDI (1.62 mL, 10.0 mmol, 2.0 equiv) under a highly pure nitrogen atmosphere. Prepolymerization was performed at 85 °C for 2.5 h with tin(II) 2-ethyl hexanoate (0.1 wt %) as the catalyst. The chain-extending reaction was followed by the addition of HPAP (1.32 g, 5 mmol, 1 equiv) at 85 °C for 4.5 h. The reaction temperature was subsequently reduced to 25 °C, and the mixture was stirred overnight. The synthesized polymer (PU–HPAP) was precipitated with distilled water at 25 °C for 48 h and dried *in vacuo* at room temperature (Figure 2).

The synthesis of PU without a chain extender was performed with the same monomer ratios (5.0 mmol or 1.0 equiv PCL diol and 10.0 mmol or 2.0 equiv HDI) and polymerization parameters with which prepolymerization was performed at 85 °C; then, the reaction was carried out overnight at 25 °C. Also, after prepolymerization, L-glutamic acid containing polyurethanes (PU–L-Glu) were also synthesized according to the same procedures described previously. For the PU–L-Glu samples, the chemical analysis (NMR and FTIR spectroscopy) results did not show any significant difference compared to the non-chain-extended PUs; this may have been due a lack of detection of glutamic acid molecules in the polymer chains by spectroscopic techniques.

Characterization

The chemical characterization of HPAP was conducted with NMR spectrometry and HRMS. NMR spectra were recorded on a Bruker DPX 400-MHz FT-NMR instrument for ^{1}H-NMR and ^{13}C-NMR, with the chemical shifts (δs) reported in parts per million and with tetramethylsilane as an internal standard with hexadeuterated dimethyl sulfoxide (DMSO-d_6) or $CDCl_3$ as the solvent. Mass spectra were obtained on an HRMS Waters SYNAPT MS.

Polymer characterizations were done in terms of the chemical properties, molecular weight, and thermal properties. ^{1}H-NMR spectroscopy investigations were conducted as given in the Results and Discussion section. The chemical functionalities of PU and PU–HPAP were characterized with an ATR–FTIR spectrometer (PerkinElmer Spectrum 65). Spectra were obtained

over a frequency range of 600–4000 cm^{-1} with 4 cm^{-1} resolutions and an average of 32 scans. The solution properties of PU and PU–HPAP were determined as the weight-average molecular weight and radius of gyration by SLS (Malvern CGS-3). The refractive index increment (dn/dc) values of the polymer solutions (concentrations = 10, 30, 40, and 50 g/dm^3 were read by a refractometer. PU films (0.5 mm thick) were prepared through the casting of PU solutions in $CHCl_3$; the samples were poured onto a polytetrafluoroethylene plate. The thermal transitions of the polymer films were conducted by DSC (PerkinElmer Diamond) at a heating rate of 10 °C/min under an N_2 flow. The thermal stability and thermal decomposition investigations of the biodegradable PU samples were achieved with TGA (PerkinElmer Pyris 1) under an N_2 atmosphere.

The surface hydrophilicities and free energies of the prepared films were studied with contact angle goniometry (KSV-CAM200). For each sample, at least 10 contact angle measurements were carried out. The test liquids, water, formamide ($HCONH_2$), and diiodomethane, were used with bromonapthalene. For each sample, at least 10 contact angle measurements were carried out. The total surface free energies (SFEs) and polar and dispersive components were calculated by the Owens–Wendt–Rabel–Kaelble method.

In Vitro Degradation Studies

To study the enzymatic degradation of the polymers, samples were prepared as equal circular discs (radius = 0.5 cm) and kept in a lipase buffer solution (0.1 mg/mL lipase in PBS) at 37 °C. The lipase degradation medium was refreshed two times per week. The degradation performances of the polymers were calculated from the percentage weight loss of the samples, determined gravimetrically (number of samples, $n = 5$). The samples were weighed (W_0) before incubation. Then, samples were removed weekly, rinsed with water three times, lyophilized, and weighed (W_1). The degradation percentage was calculated through the percentage weight loss with the following equation:

$$\%\ \text{Weight loss} = \frac{W_0 - W_1}{W_0} \times 100 \quad (1)$$

In addition, the degradation morphologies of the polymers were observed by scanning electron microscopy (SEM; FEI Quanta 400F, Holland). Sputter coating with an Au thin film was carried on the samples for SEM investigations.

Cytotoxicity Assay

The cytotoxicities of the polymers were tested with the standard ISO10993-5 ("Biological Evaluation of Medical Devices—Part 5: Tests for *In Vitro* Cytotoxicity—Indirect MTT Cytotoxicity Test"). The L929 mouse fibroblast (ATCC NCTC clone 929: CCL 1) cell line was used throughout the experiments. Briefly, samples were kept in cell culture medium with a 6 cm^2/mL surface/medium ratio at 37 °C for 72 h (% 5 CO_2 and >% 90 humidity atmosphere). The content of the cultivation medium included 90% Dulbecco's modified Eagle's medium and 10% fetal bovine serum with 1% L-glutamine and 1% penicillin/streptomycin. L929 cells were seeded into 96 well plates with 1 × 10^5 cells/mL densities in each well. After 72 h of incubation, the incubated mediums were interacted with L929 cells. The cell medium was used as a negative control, whereas cell medium with 10% DMSO was used as a positive control. After 24 h of incubation, to measure the mitochondrial activity, an MTT assay was performed (number of samples, $n = 5$). A mixture of 10% MTT (5 mg/mL) reagent and 90% culture medium was added to each well and incubated at 37 °C for 4 h. After the incubation period, the culture medium was removed, and 100 µL of propan-2-ol/0.04 *M* HCl mixture was added to dissolve the metabolized MTT reagent. The absorbance of formazan crystals was measured at 570 nm with an enzyme-linked immunosorbent assay microplate reader, and the cell viability index was calculated.

Statistical Analysis

A one-way analysis of variance test was used for statistical analysis, and the differences in the statistical examinations were performed by a Tukey test ($p < 0.05$ was considered statistically significant).

RESULTS AND DISCUSSION

HPAP and HPAP-based PU were successfully synthesized, and the obtained results are discussed in the following section.

Chemical Characterization of HPAP

The chemical characterization of HPAP was performed by the ^{1}H-NMR, HRMS, and FTIR spectroscopy techniques with the following results:

^{1}H-NMR (400 MHz, DMSO-d_6, δ): 5.03 (s, 2H, NH_2), 4.18 (m, 4H, CH_2), 3.84 (m, 2H, C*H*), 4.46 (s, 2H, O*H*), 3.41 (t, 1H, C*H*), 2.15 (m, 2H, CH_2), 2.02 (m, 2H, CH_2), 0.98 (d, 6H, $J = 4.0$ Hz, CH_3). ^{13}C-NMR (100 MHz, DMSO-d_6,δ): 177.73 (*C*═O), 172.44 (*C*═O), 70.12 (O*C*H_2), 64.52 (*C*HOH), 54.88 (*C*HNH_2), 29.07 (*C*H_2), 28.76 (*C*H_3), 28.45 (*C*H_2). FTIR spectroscopy (cm^{-1}): HRMS (EI) Calcd for $C_{11}H_{22}NO_6$ (M^+H^+), 264.1443; found, 264.1447.

These results confirm that the obtained product was mainly HPAP.

Chemical and Thermal Properties of the PUs

The PUs were synthesized by a two-step condensation reaction of PCL diol and HDI components either with the presence of HPAP or without chain extender (Figure 2). The presence of excess HDI ensured that the prepolymer had isocyanate-ending chains. For the non-chain-extended synthesis, the excess isocyanate caused additional further secondary reactions, which resulted in the formation of allophanate and biuret groups, which affected the properties of the PUs in terms of chemistry, solubility, and biodegradability. During the reactions, great care was given to removing excess moisture to prevent undesirable secondary reactions. HPAP was introduced into the polymerization system after prepolymer formation, and PU–HPAP synthesis was carefully carried out at a low temperature to prevent degradation of the glutamic acid derived HPAP. We proposed a mechanism for the amino and hydroxyl functional groups of HPAP reacting with the isocyanate ends of the prepolymer. ^{1}H-NMR confirmed the molecular structure of the synthesized PU and PU–HPAP, which are shown in Figure 3. The ^{1}H-NMR spectrum of the monomer PCL diol is also given to clarify the structure of the polymers [Figure 3(a)]. The PU–HPAP

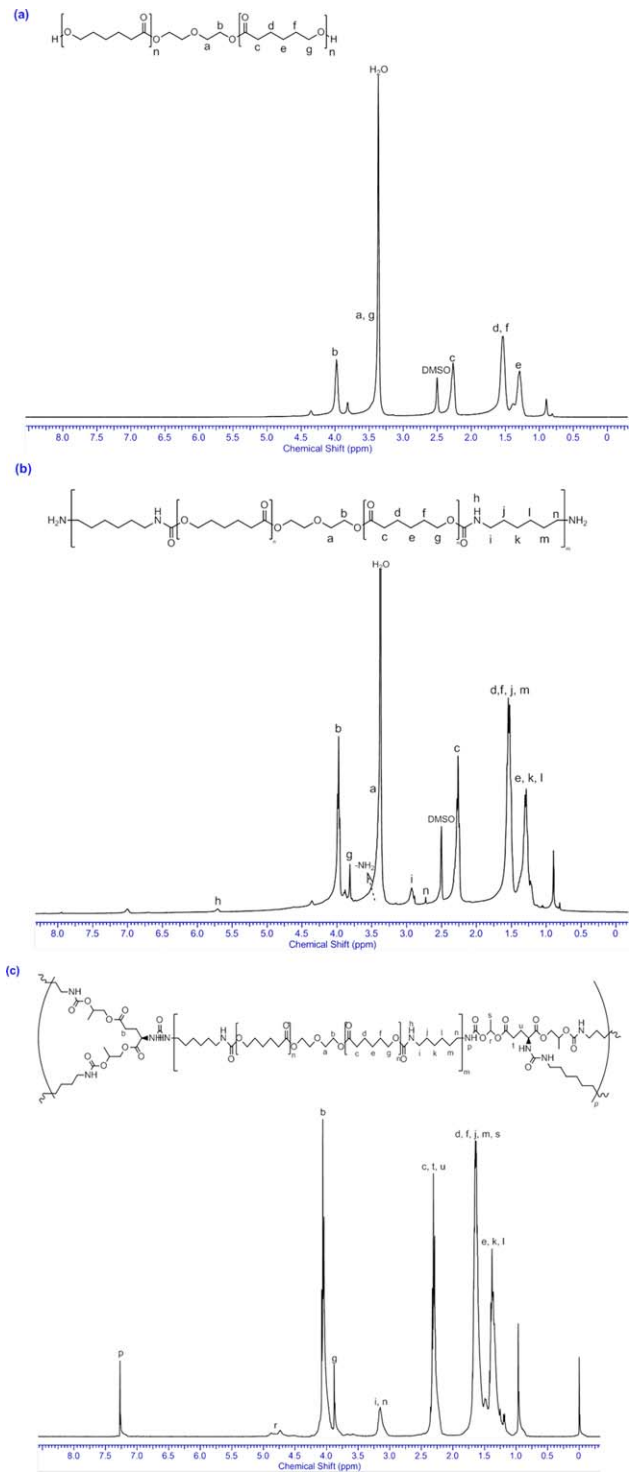


Figure 3. ^{1}H-NMR spectra of (a) PCL diol, (b) PU, and (c) PU–HPAP. [Color figure can be viewed at wileyonlinelibrary.com]

exhibited peaks at 1.38, 1.63, 2.30, and 3.98 ppm, which were attributed to the methylene protons [Figure 3(c)]. The sharp peak at 7.27 ppm was attributed to the amide proton of —N*H*COO— in the chain extender. Also, the sharp peak at 2.30 ppm showed the methylene protons of —COOCH_2CH_2CHNHCOO—. An alcohol and amino group ended the longer side chain of the novel chain extender and could provide new active reaction sites for the development of multifunctional biodegradable PUs.

The FTIR spectra of the PCL diol, PU, and PU–HPAP samples exhibited the two typical stretching vibrations at 3300 and 1726–1705 cm^{-1} for PUs (Figure 4). The ATR spectra showed

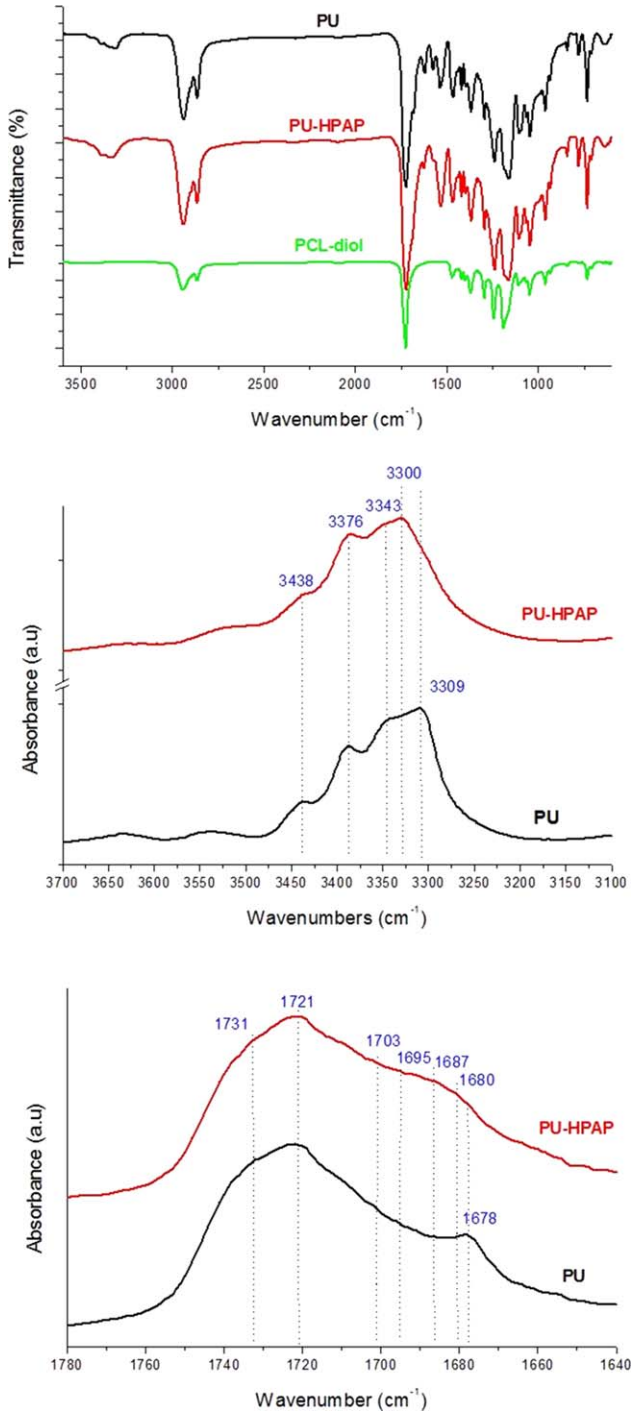


Figure 4. ATR–FTIR spectra of the PCL diol, PU, and PU–HPAP (4000–600 cm^{-1}). The N—H and C═O vibration stretching regions of PU and PU–HPAP are shown. [Color figure can be viewed at wileyonlinelibrary.com]

Table I. Characteristic IR Absorption Frequencies for the C=O and N—H Groups in the PUs

Group	Mode	Frequency (cm^{-1})
N—H	Free	3448, 3376
N—H	Stretching, H bonded	3343, 3300
C—H	Asymmetrical stretching	2940
C—H	Symmetrical stretching	2864
C=O	Stretching	1716
C=O (urethane)	C=O...H—N	1740-1680
C=O (urethane)	C=O...H—N	1680-1695 (ordered)
C—O—C	Stretching	1230
C—O	Stretching	1075

Table II. Weight-Average Molecular Weights and Solution Properties of the PUs

Sample	Weight-average molecular weight (g/mol)	Radius of gyration (nm)
PU	4.793×10^4	133.8
PU-L-Glu	1.310×10^5	180.1
PU-HPAP	3.311×10^4	142.0

no free isocyanate at 2270 cm^{-1}; this indicated complete polymerization. In the ATR spectra of PU and PU–HPAP, the band at 3300 cm^{-1} corresponded to NH stretching vibrations in the presence of hydrogen bonding.[33] Two stretching bands at 2940 and 2864 cm^{-1} corresponded to C—H asymmetrical and symmetrical stretching in $—CH_3$, respectively. C=O stretching bands were observed at 1716 cm^{-1} in the FTIR spectra of the PUs. Very sharp peaks at 1075 and 1230 cm^{-1} represented urethane or C—O stretching and C—O—C vibrations. The N—H and C=O groups of PU formed hydrogen bonds between the polymer chains; this significantly affected the properties of the PUs.[33] Hydrogen bonds were confirmed from NH and the carbonyl stretching region in Figure 4. According to the literature, non-hydrogen-bonded (free) urethane carbonyls give a sharp peak in the 1730–1740 cm^{-1} range, and strongly hydrogen-bonded and ordered carbonyl peaks (C=O...H—N) are in the 1680–1695 cm^{-1} range.[34] Ordered and hydrogen-bonded C=O...H—N peaks were observed for PU–HPAP because of the presence of the chain extender. Depending on the hydrogen bonding, other urethane C=O peaks were also observed between 1740 and 1680 cm^{-1}. So, we concluded that the chain extender HPAP dramatically controlled H bonding. PU–HPAP had N—H—N—H ordered bonds at 3300 cm^{-1}, hydrogen-bonded N—H stretching at 3343 cm^{-1}, and hydrogen-bonded C=O stretching between 1680 and 1895 cm^{-1}. The characteristic IR absorption frequencies observed for C=O and N—H groups in PUs are also summarized in Table I.

The solution properties of the samples were analyzed by SLS. Samples were dissolved in DMF with five different concentrations (10, 30, 40, and 50 g/dm^3, and the refractive index increment (dn/dc) values were measured with a refractometer. The average scattering intensity lead to the particle weight-average molecular weight and radius of gyration. The radius of gyration is the root mean square distance of a chain end to a polymer's center of gravity. The data obtained from the Berry plots of SLS are tabulated in Table II.

The non-chain-extended PU had a weight-average molecular weight value of 47,930 g/mol, and with the presence of HPAP, the weight-average molecular weight decreased to 33,110 g/mol (PU–HPAP). This decrease was most probably due to the presence of HPAP at the polymer chain ends. Similarly, as reported in the literature,[21] the presence of an amino acid based chain extender, L-phenylalanine ester, resulted a decrease in the molecular weight of PU. Also, L-arginine, glycine, L-aspartic acid, and butane diamine amino as chain extenders provided different differences in PU molecular weights.[23] Alcohol and amino group ending side chains on the novel chain extender could also provide new active reaction sites for the development of multifunctional biodegradable PUs. The synthesis of PU in L-Glu media mostly catalyzed the polymerization, and the weight-average molecular weight was found to be 131,000 g/mol from the Berry plot (it was also found as 61,400 g/mol from the Guinier plot of SLS). The thermal transitions of the PUs, which were investigated by DSC, are tabulated in Table III.

As expected, the first and second run heating profiles of DSC analysis differed because of the segmental orientation changes of the polymers. The second heating results show that PU–HPAP had the highest glass-transition temperature (T_g) value of −48.74 °C among all of the samples. The presence of the HPAP chain extender between the main polymer chains restricted the segmental motion and resulted a slight increase in T_g. The FTIR spectroscopy results prove that PU–HPAP had hydrogen-bonded N—H stretching and C=O stretching vibrations, and these H bonds resulted an increase in T_g. In the literature,[27,35]

Table III. Thermal Transitions of the PU Samples Obtained by DSC

Sample	T_g for the first heating (°C)	T_m for the first heating (°C)	ΔH (J/g)	Cooling (°C)	T_g for the second heating (°C)	T_m for the second heating (°C)	ΔH (J/g)
PU	−56.30	43.90	39.79	2.29	−50.09	36.24	33.18
PU-L-Glu	−53.63	31.73	35.14	−8.05	−51.63	34.77	34.12
PU-HPAP	−50.03	44.23	52.66	−5.27	−48.74	34.96	32.98

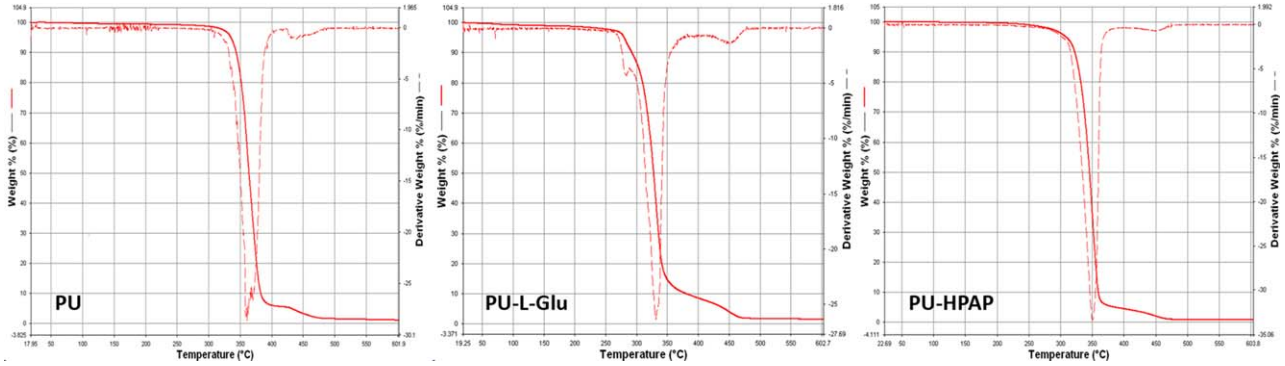


Figure 5. TGA thermograms of PU, PU–L-Glu, and PU–HPAP. [Color figure can be viewed at wileyonlinelibrary.com]

there have been several articles reporting slight increases in T_g after the incorporation of chain extenders into the polymer structure. PU and PU–L-Glu had T_g values of −50.09 and 51.63 °C, respectively. Also, a melting temperature (T_m) was observed for all samples; this was an indication of the presence of crystalline domains in PU, PU–L-Glu, and PU–HPAP chains. In the first run, the T_g values of PU and PU–HPAP were higher than body temperature (37 °C), and after the second run, T_g values of 36.24 °C for PU and 34.96 °C for PU–HPAP were obtained. The melting enthalpy (ΔH) value determined from the second heating scan of PU–HPAP (32.98 J/g) was lower than the ΔH obtained from the first heating (52.66 J/g). The same trend was observed for the ΔH values of PU and PU–L-Glu. In the literature, during the second heating scan, similar decreases in ΔH were observed for chain-extended PUs.[36]

The thermal degradation profiles of PU, PU–HPAP, and PU–L-Glu were investigated by TGA, and the thermograms are shown in Figure 5. Two-step thermal degradation profiles were obtained for PU, PU–HPAP, and PU–L-Glu showed a three-step thermal degradation profile. As shown in the literature, hard-segment urethane degradation occurs either by depolycondensation to alcohol and isocyanate or cleavage of the C═O bond of urethane. Azzam *et al.*[34] worked on the thermogravimetric degradation of PU and concluded that the first weight loss attributed to hard-segment degradation and the weight losses in the second and third steps were proportional to the soft-segment content. PU, PU–L-Glu, and PU–HPAP had thermal stability up to 300, 270, and 250 °C, respectively. The pristine PU showed its first weight loss over 350 °C, and soft-segment degradation occurred around 440 °C. The first weight loss of PU–L-Glu was around 275 °C and was due to the degradation of L-Glu. Also, the hard-segment degradation of PU–L-Glu was observed around 330 °C. For PU–HPAP, a two-step thermogravimetric degradation profile was observed, in which the first weight loss at 350 °C was attributed to hard-segment degradation and the polyester-based soft segment degraded at 450 °C.

Biodegradation Properties of the PUs

The PU degradation rate and mechanism depends on the monomer type, molecular weight, polydispersity, crystallinity, tacticity, hydrophilic or hydrophobic functional groups, and susceptibility under *in vivo* conditions.[16] In light of this knowledge, the enzymatic degradation of the ester backbone was investigated extensively in lipase-containing medium at 37 °C.

The degradation performances of PU, PU–L-Glu, and PU–HPAP were calculated as percentage weight losses and are given in Figure 6. The HPAP-based PU had about 20, 25, and 75% weight losses after 7, 14, and 35 days, respectively. However, PU and PU–L-Glu did not show any biodegradation profiles at 35 days. These results prove that the addition of HPAP chain extender into PU macromolecule accelerated the biodegradation behavior of the polymer. In the literature, markedly faster degradations

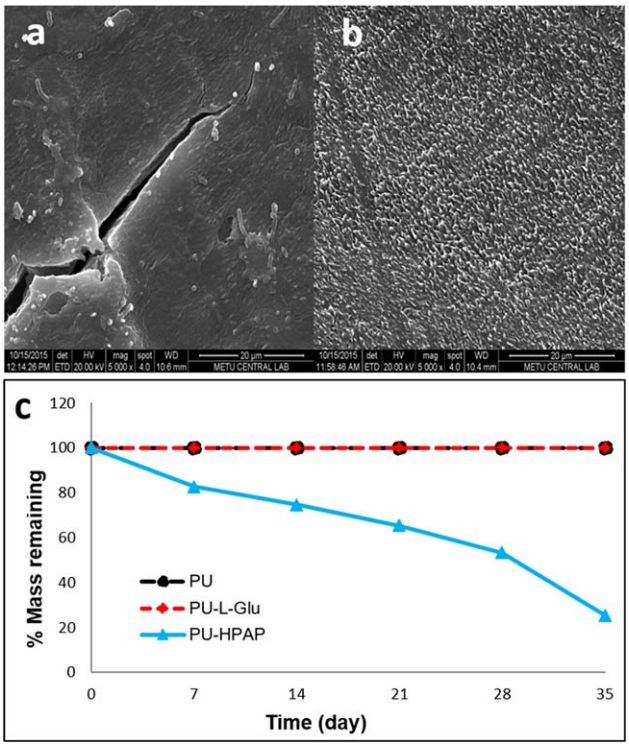


Figure 6. SEM images showing the *in vitro* enzymatic degradation morphologies of (a) PU and (b) PU–HPAP on the 7th day. Bulk degradation of PU started, whereas PU–HPAP had surface-erosion-type degradation. (c) *In vitro* degradation profiles of PU, PU–L-Glu, and PU–HPAP in the presense of lipase media at 37 °C for a 5-week period. [Color figure can be viewed at wileyonlinelibrary.com]

Table IV. Water Contact Angles and SFE Values for the PUs

Sample	Water contact angle	Total SFE: γ_s (mN/m)	Dispersive component of SFE: γ_s^d (mN/m)	Polar component of SFE: γ_s^d (mN/m)
PU	91.6 ± 2.2	49.6	49.5	0.1
PU–L-Glu	77.0 ± 1.0	47.7	45.4	2.3
PU–HPAP	66.5 ± 1.8	51.9	45.3	6.6

were obtained for PUs with the presence of the amino acid based diester chain extender.[21,22] Skarja and Woodhouse[21] reported that the incorporation of L-phenyl alanine based diester as the chain extender into the PU structure imparted a particular susceptibility toward enzymatic attack rather than simple hydrolysis. Chan-Chan *et al.*[23] prepared degradable segmented poly(urea)urethanes with the amino acids L-arginine, glycine, and L-aspartic acid as chain extenders, and these polymers degraded slowly in PBS at pH 7.4, but degradation accelerated in acidic, alkaline, and oxidative media. It is well known that the biodegradation of a polymer can be classified as bulk degradation and surface-erosion-type degradation. In the literature, the biodegradation morphologies of polymers have mostly been investigated by SEM.[28,36] The morphologies after 7 days showed that the PU sample had cracks on the surface [Figure 6(a)]. Similar morphologies have also been observed in the literature for biodegradable PUs.[28,32]

On the other hand, surface erosion was observed for PU–HPAP after 7 days; this implied that water diffusion into the matrix was slower than hydrolysis [Figure 6(b)]. In a manner similar to that found in Skarja and Woodhouse's work,[21] enzymatic attack appeared to be surface-limited, and surface erosion morphology was observed for the HPAP chain-extended PU. Also, after 35 days, the bulk degradation of PU–HPAP began. Similar morphologies were observed by Báez et al.;[36] this implied that the synthesis of poly(ester urethane amide)s from α,ω-telechelic poly(ε-caprolactone) diols and 1,6-HDI with three different

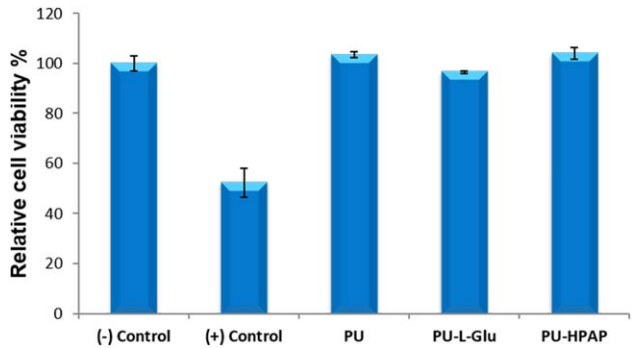


Figure 7. *In vitro* cytotoxicity test results by an indirect MTT assay with the L929 cell line. The bars indicate the relative cell viability of the negative and positive control groups and the synthesized PU, PU–L-Glu, and PU–HPAP polymers on the indirect MTT assay. The positive control showed a statistically significant decrease (~50%) in the cell viability for L929 fibroblast cells ($p < 0.05$), whereas PU, PU–L-Glu, and PU–HPAP showed no significant difference against the negative control group. [Color figure can be viewed at wileyonlinelibrary.com]

diamide−diol chain extenders degraded hydrolytically at very long times by surface erosion.

To clarify the surface erosion of PU–HPAP, the surface hydrophilicities and free energies were examined with a contact angle goniometer. The SFEs (calculated by the Owens–Wendt–Rabel–Kaelble method) and water contact angles are tabulated in Table IV. PU–HPAP showed the highest hydrophilicity among all of the samples.

The contact angle values were found to be 91° for PU, 77° for PU–L-Glu, and 66.5° for PU–HPAP. The chemistry of HPAP introduced more functional groups and resulted in an increase in the hydrophilicity. We concluded that the increase in the hydrophilicity triggered the surface erosion, and the penetration of water molecules through the surface of PU–HPAP was favored. Also, more energetic surfaces were obtained with the presence of HPAP. The total SFEs were found to be 51.9, 49.6, and 47.77 mN/m for PU–HPAP, PU, and PU–L-Glu, respectively. It was also proven that the polar component of the SFE was found to be highest for PU–HPAP (6.6 mN/m) compared to PU (0.1 mN/m) and PU–L-Glu (2.3 mN/m). The presence of HPAP resulted in more polar groups in PU and a more hydrophilic polymer that was susceptible to hydrolytic degradation.

Biocompatibility Results of the PUs

The *in vitro* cytotoxicity test results show that the positive control group showed a statistically significant decrease (~50%) against the negative control; in contrast, the synthesized PU, PU–L-Glu, and PU–HPAP polymers had no significant effect on the cell viability (Figure 7) for the L929 cell line. About 100% cell viability was observed for the PU, PU–L-Glu, and PU–HPAP polymers. The addition of HPAP into the PU segment did not affect the biocompatibility of the polymer. As a result, PU, PU–L-Glu, and PU–HPAP did not leach toxic residue or degradation products into the biological environment.

CONCLUSIONS

The design of new biodegradable PUs is crucial with the growing intensity of tissue engineering and regenerative medicine. In this study, a novel chain extender, HPAP, was successfully synthesized with L-Glu and reacted with a PU prepolymer during the second step of the polycondensation reaction. Chemical characterizations proved the chemical binding between HPAP and PU. HPAP chain extension increased the T_g and T_m values of the polymer and resulted in a more hydrophilic and energetic surface. During *in vitro* degradation studies, PU–HPAP showed surface erosion with a 20% weight loss on the 7th day, and after 35 days, 75% of the HPAP-based PU degraded via bulk

degradation. We concluded that the biodegradation PU could be tuned by the addition of HPAP as a chain extender into the PU hard segment. The biodegradable PU–HPAP showed promising outcomes for tissue engineering scaffolds and drug-delivery systems for surface-erosion-based release mechanisms.

ACKNOWLEDGMENTS

This research was supported by Hacettepe University Scientific Research Projects Coordination Unit with Grant No 014 D10 301 001-718.

REFERENCES

1. Janik, H.; Marzec, M. *Mater. Sci. Eng. C* **2015**, *48*, 586.
2. Aksoy, E. A.; Sezer, U. A.; Kara, F.; Hasirci, N. *J. Biomater. Tissue Eng.* **2015**, *5*, 104.
3. Calamak, S.; Aksoy, E. A.; Ertaş, N.; Erdogdu, C.; Sagıroglu, M.; Ulubayram, K. *Eur. Polym. J.* **2015**, *67*, 99.
4. Aydemir Sezer, U.; Arslantunali, D.; Aksoy, E. A.; Hasirci, V.; Hasirci, N. *J. Appl. Polym. Sci.* **2014**, *131*, DOI: 10.1002/app.40110.
5. Hong, Y.; Ye, S.-H.; Pelinescu, A. L.; Wagner, W. R. *Biomacromolecules* **2012**, *13*, 3686.
6. Gultekinoglu, M.; Oh, Y. J.; Hinterdorfer, P.; Duman, M.; Çatçat, D.; Ulubayram, K. *RSC Adv.* **2016**, *6*, 17092.
7. Xing, Q.; Li, R.-B.; Zhang, X.-Q.; Zhang, L.-Y.; Wang, D.-J. *Chin. J. Polym. Sci.* **2015**, *33*, 1294.
8. Niu, Y.; Zhu, Y.; Gao, R.; Yu, W.; Li, L.; Xu, K. *J. Inorg. Organomet. Polym. Mater.* **2015**, *25*, 81.
9. Hasirci, N.; Aksoy, E. A. *High Perform. Polym.* **2007**, *19*, 621.
10. Alishiri, M.; Shojaei, A.; Abdekhodaie, M.; Yeganeh, H. *Mater. Sci. Eng. C* **2014**, *42*, 763.
11. Aksoy, E. A.; Hasirci, V.; Hasirci, N.; Motta, A.; Fedel, M.; Migliaresi, C. *J. Bioact. Compat. Polym.* **2008**, *23*, 505.
12. Gultekinoglu, M.; Sarisozen, Y. T.; Erdogdu, C.; Sagiroglu, M.; Aksoy, E. A.; Oh, Y. J.; Hinterdorfer, P.; Ulubayram, K. *Acta Biomater.* **2015**, *21*, 44.
13. Kara, F.; Aksoy, E. A.; Calamak, S.; Hasirci, N.; Aksoy, S. *J. Bioact. Compat. Polym. Biomed. Appl.* **2016**, *31*, 72.
14. Gultekinoglu, M.; Kurum, B.; Karahan, S.; Kart, D.; Sagiroglu, M.; Ertaş, N.; Ozen, A. H.; Ulubayram, K. *Mater. Sci. Eng. C* **2017**, *71*, 1166.
15. Podporska-Carroll, J.; Ip, J. W.; Gogolewski, S. *Acta Biomater.* **2014**, *10*, 2781.
16. Sobczak, M. *Polym.-Plast. Technol. Eng.* **2015**, *54*, 155.
17. Tatai, L.; Moore, T. G.; Adhikari, R.; Malherbe, F.; Jayasekara, R.; Griffiths, I.; Gunatillake, P. A. *Biomaterials* **2007**, *28*, 5407.
18. Cui, H.; Zhuang, X.; He, C.; Wei, Y.; Chen, X. *Acta Biomater.* **2015**, *11*, 183.
19. Chen, K.-J.; Tang, L.; Garcia, M. A.; Wang, H.; Lu, H.; Lin, W.-Y.; Hou, S.; Yin, Q.; Shen, C. K.-F.; Cheng, J. *Biomaterials* **2012**, *33*, 1162.
20. Curtis, D. R.; Watkins, J. C. *Nature* **1961**, *191*, 1010.
21. Skarja, G.; Woodhouse, K. *J. Biomater. Sci. Polym. Ed.* **2001**, *12*, 851.
22. Skarja, G.; Woodhouse, K. *J. Biomater. Sci. Polym. Ed.* **1998**, *9*, 271.
23. Chan-Chan, L.; Tkaczyk, C.; Vargas-Coronado, R.; Cervantes-Uc, J.; Tabrizian, M.; Cauich-Rodriguez, J. *J. Mater. Sci.: Mater. Med.* **2013**, *24*, 1733.
24. Xu, C.; Huang, Y.; Wu, J.; Tang, L.; Hong, Y. *ACS Appl. Mater. Interfaces* **2015**, *7*, 20377.
25. Domanska, A.; Boczkowska, A. *Polym. Degrad. Stab.* **2014**, *108*, 175.
26. Baheiraei, N.; Yeganeh, H.; Ai, J.; Gharibi, R.; Azami, M.; Faghihi, F. *Mater. Sci. Eng. C* **2014**, *44*, 24.
27. Zhang, C.; Zhang, N.; Wen, X. *J. Biomed. Mater. Res. B* **2006**, *79*, 335.
28. Tsou, C.-H.; Lee, H.-T.; Tsai, H.-A.; Cheng, H.-J.; Suen, M.-C. *Polym. Degrad. Stab.* **2013**, *98*, 643.
29. Chan-Chan, L. H.; Solis-Correa, R.; Vargas-Coronado, R. F.; Cervantes-Uc, J. M.; Cauich-Rodriguez, J. V.; Quintana, P.; Bartolo-Perez, P. *Acta Biomater.* **2010**, *6*, 2035.
30. Sarkar, D.; Yang, J. C.; Gupta, A. S.; Lopina, S. T. *J. Biomed. Mater. Res. A* **2009**, *90*, 263.
31. Ma, Y.; Liu, J.; Luo, M.; Xing, J.; Wu, J.; Pan, H.; Ruan, C.; Luo, Y. *RSC Adv.* **2017**, *7*, 13886.
32. Wu, C.-L.; Chiu, S.-H.; Lee, H.-T.; Suen, M.-C. *Polym. Adv. Technol.* **2016**, *27*, 665.
33. Aksoy, E. A.; Hasirci, N. *J. Biomater. Tissue Eng.* **2012**, *2*, 345.
34. Azzam, R. A.; Mohamed, S. K.; Tol, R.; Everaert, V.; Reynaers, H.; Goderis, B. *Polym. Degrad. Stab.* **2007**, *92*, 1316.
35. Gorna, K.; Polowinski, S.; Gogolewski, S. *J. Polym. Sci. Part A: Polym. Chem.* **2002**, *40*, 156.
36. Báez, J. E.; Ramírez, D.; Valentín, J. L.; Marcos-Fernández, Á. *Macromolecules* **2012**, *45*, 6966.